JOURNAL OF AGRICULTURAL AND FOOD CHEMISTRY

Alkali Extraction of β-D-Glucans from *Saccharomyces cerevisiae* Cell Wall and Study of Their Adsorptive Properties toward Zearalenone

ALEXANDROS YIANNIKOURIS,[†,‡] JEAN FRANÇOIS,[§] LAURENT POUGHON,[⊥] CLAUDE-GILLES DUSSAP,[⊥] GÉRARD BERTIN,[‡] GEORGES JEMINET,[#] AND JEAN-PIERRE JOUANY*[,†]

UR1053 INRA, Unité de Recherches sur les Herbivores Centre de Clermont-Theix, 63122 St-Genès Champanelle, France; UMR-CNRS 5504, UR-INRA 792, INSA, 135 avenue de Rangueil, 31077 Toulouse Cedex 4, France; Laboratoire de Génie Chimique et Biologique, CUST, Université Blaise Pascal—Clermont-Ferrand II, 24 avenue des Landais, 63174 Aubière Cedex, France[1]

The isolated cell wall of *Saccharomyces cerevisiae* has some capacity to adsorb zearalenone (affinity near 30%) and reduce the bioavailability of toxins in the digestive tract. The adsorption process was quantified in vitro, and the data obtained when plotted with Hill's equation indicated a cooperative process. The model showed that the adsorption capacity was related to the yeast cell wall composition. This work focused on the role of various β-D-glucan types in the efficacy of zearalenone adsorption by yeast cell wall and sought to elucidate some of the adsorption mechanisms. Zearalenone was mixed at 37 °C with a constant quantity of alkali-soluble or alkali-insoluble β-D-glucans isolated from yeast cell walls, and the amount of adsorbed zearalenone was measured. Given that the alkali solubility of β-D-glucans is a determining factor for their three-dimensional conformation and that the alkali-insoluble fraction had a greater affinity (up to 50%) than the alkali-soluble fraction (∼16%), it was concluded that the three-dimensional structure strongly influences the adsorption process. The alkali insolubility of β-D-glucans led to the formation of single and/or triple helices, which have been identified as the most favorable structures for zearalenone adsorption efficacy. The β(1,3)-D-glucan and β-(1,6)-D-glucan compositions of the two alkali-extracted fractions and their involvement in the adsorption process are discussed.

KEYWORDS: Zearalenone; mycotoxins; yeast cell wall; alkali-soluble β-D-glucans; alkali-insoluble β-D-glucans; adsorption; cooperativity; detoxification

INTRODUCTION

Zearalenone (ZEN), 6-(10-hydroxy-6-oxo-*trans*-1-undecenyl)-β-resorcylic acid lactone, is a nonsteroidal mycotoxin produced by numerous *Fusarium* species. Toxicological risks for humans can arise from direct contamination of grains (wheat, barley, grain sorghum, and corn), grain products (flour, bread, and processed commercial feed), and fruits or by carry-over into milk and edible animal tissues (*1*). Because fusariotoxins occur in a wide range of agricultural commodities pre- or postharvest, and also during transport and storage, ZEN is potentially harmful to both animals and humans (*2*).

ZEN is responsible for premature puberty syndrome in children in epidemic proportions in Puerto Rico (*3*). Evidence has been found of interactions of ZEN with the endocrine system in which endocrine metabolites modulate biological response to ZEN (*4*). However, little other conclusive information is available regarding its effects on humans (*1*).

Major effects of ZEN have been evidenced in farm and laboratory animals (dairy cattle, turkeys, lambs, rats, mice, guinea pigs, and especially swine), on the urogenital system, and have been characterized by hyperestrogenism at dietary concentrations of ≥1.0 ppm (*5*, *6*). Estrogenic effects lead to the atrophy of testicles and ovaries, enlargement of mammary glands, abortion, and, in severe cases, impaired reproductive cycle, conception, ovulation, fetal implantation, and development, leading to infertility (*7*). ZEN and its analogues also

* Author to whom correspondence should be addressed [telephone + 33 (0)4 73 62 40 54; fax + 33 (0)4 73 62 46 59; e-mail jouany@clermont.inra.fr].
† UR1213 INRA, URH, Centre de Clermont-Theix, France.
‡ Present address: Alltech-France, 2−4 Avenue du 6 Juin 1944, 95190 Goussainville, France.
§ UMR-CNRS 5504, UR-INRA 792, INSA, Toulouse, France.
⊥ Laboratoire de Génie Chimique et Biologique, Université Blaise Pascal, Clermont-Ferrand, France.
UMR-CNRS 6504, Laboratoire de Synthèse et Étude des Systèmes à Intêret Biologique, Université Blaise Pascal, Clermont-Ferrand II, 63177 Aubière Cedex, France.

10.1021/jf035127x CCC: $27.50
Published on Web 05/05/2004

produce immunotoxic effects by inhibiting mitogen-stimulated lymphocyte proliferation (*8*) and inducing thymic atrophy and macrophage activation (*9*).

In addition to the complexity of the toxicology of mycotoxins, due to their multiple nature, pathways, and effects, synergistic effects among mycotoxins are commonly observed in multi-contaminated foods, making it difficult to clarify the real causes of mycotoxicosis. Thus, the true impact of these mycotoxins on animal and human health has not been clearly established.

Keeping mycotoxins out of the food chain requires practical and effective strategies for their management. Despite the use of recommended agricultural practices to avert mold development and mycotoxicogenesis during crop growth, harvesting, and storage, contamination still occurs (*1*). Strategies involving removal (*10*, *11*) and/or destruction of contaminated food and feed (*12*, *13*) are unrealistic because of their economic costs. A new strategy has emerged during the past decade that makes use of various binding agents or sorbents (*1*). Inorganic compounds such as clays, bentonites, and aluminosilicates and organic compounds such as yeast or bacterial cell walls have the ability to complex some mycotoxins (*14*, *15*). Addition of such adsorbents to food and feeds contaminated by mycotoxins reduces their bioavailability in the digestive tract and their detrimental effects on animals. Furthermore, the carry-over of parent toxin and toxic metabolites into edible animal products is reduced, protecting consumers from toxic hazard (*16*).

Previous in vitro studies have shown that β-D-glucans extracted from the cell wall of *Saccharomyces cerevisiae* adsorb ZEN from aqueous solution (*16*). The cell wall is a prominent distinguishing feature of all yeasts, providing physical protection and osmotic support. The mechanical strength of the wall is due mainly to the inner layer, which consists of β-D-glucans [β(1,3)- and β(1,6)-D-glucans] and chitin; together they represent 50−60% of the wall dry weight. The outer layer is made of heavily glycosylated mannoproteins, which are involved in cell−cell recognition events and limitation of wall porosity (*17*, *18*). Yiannikouris et al. (*16*) showed in vitro that adsorption of ZEN is correlated to the amount of β-D-glucans contained in yeast cell wall ($R^2 = 0.889$), whereas chitin stiffened the cell wall structure and restricted access of ZEN to the chemical sites of the β-D-glucans.

To fully clarify the type of adsorption occurring between β-D-glucans and ZEN and to identify the mechanisms involved, the cell wall of four strains of *S. cerevisiae* differing in a wide range of glucan/mannan ratio and in cell wall chitin content were isolated. Because β-D-glucans from whole cell walls display strong adsorption of ZEN molecules (*16*), we used alkali treatment to isolate soluble and insoluble β-D-glucan fractions free of mannan and chitin from yeast cell walls, to improve adsorption and eliminate artifacts induced by the presence of mannans and/or chitin. Each of these fractions was tested for its ability to complex ZEN using an original in vitro technique and modeling of the data using Hill's model, which gave the most accurate parameters when compared to sigmoid or isothermal equations and provided reliable biological interpretation of the physical and chemical mechanisms involved in the complexation process (*19*). This approach differs from the usual ways of investigating surface adsorption, which generally involve multiple isothermal equations based mainly on the Langmuir equation (*20*). Calculated parameters were used to highlight the role of each fraction of β-D-glucans in the adsorption. Hypotheses concerning the role of the β-D-glucan three-dimensional (3D) structure in the ZEN adsorption process are put forward.

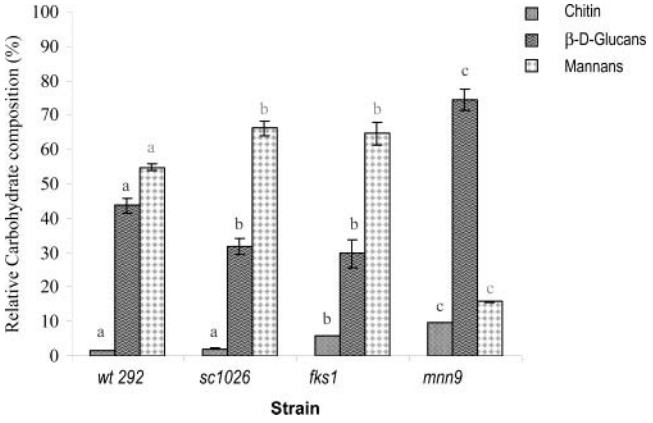

Figure 1. Percentages of monosaccharides released from acid hydrolysis of cell walls of the four yeasts tested (*16*). For each component, bars with different letters were significantly different ($p < 0.05$). Chitin was evaluated by an enzymatic method using zymolyase and chitinase.

MATERIALS AND METHODS

Apparatus, Chemical Reagents, and Biological Material. *S. cerevisiae* strain *1026* (*sc1026*) was supplied by Alltech Inc. (Nicholasville, KY). Strains *wt292*, *fks1*, and *mnn9* originated from the UMR−CNRS 5504 laboratory, UR−INRA 792, INSA, Toulouse, France.

A stock solution of ZEN (Sigma Chemical Co., St. Louis, MO) was prepared at 8.72 mM in 100% acetonitrile and stored at −20 °C. All organic solvents were of HPLC grade (Carlo Erba Reagenti, Milan, Italy). The water used in all of the experiments was prepared by processing deionized water through a Milli-Q^{uf+} system.

Production of Yeast Biomass. Four strains of *S. cerevisiae* were used: the wild type *wt292*; the *fks1* mutant type, which was deficient in β(1,3)-D-glucan synthase; the *mnn*9 mutant type, which was deficient in the gene required for N-glycosylation; and *sc1026* originating from a brewery. Yeast cells were grown in a mixture of peptone, yeast extract, and dextrose medium [YPD; 1% (w/v) yeast extract, 2% (w/v) bacteriological peptone, and 2% (w/v) glucose] in flasks, at 30 °C, shaken at 200 rpm. Yeast cultures were stopped at 2×10^7 cells/mL for cell wall extraction.

Cell Wall Characteristics (Figure 1). Mannan/glucan ratios were 1.25, 2.09, 2.18, and 0.21 in the cell walls of *wt292*, *fks1*, *sc1026*, and *mnn9*. Both *mnn9* and *fks1* presented high chitin contents, of 9.7 and 5.8%, respectively, against ∼2% for *wt292* and *sc1026*. The *sc1026* strain presented the same cell wall composition as *fks1* (*16*).

Alkali Extraction of Carbohydrates from Yeast Cell Wall (Figure 2). Yeast cells were disrupted by shaking in a mini-bead beater shaker (Mikro-Dismembrator S, B. Braun Biotech GmbH Int., Melsungen, Germany) with glass beads ("micro method") (*21*). Yeast cell walls were hydrolyzed with 2 N H_2SO_4 at 100 °C for 4 h according to the method of Dallies et al. (*22*). The extraction method was adapted from those of Fleet (*23*) and Catley (*24*), who both used NaOH for 6 h at 75 °C for extraction under nitrogen conditions. In our study, cell walls were fractionated by alkali extraction with 1 M NaOH and 0.5% of $NaBH_4$ for 24 h at 37 °C under agitation. The process became optimal when the [cell wall/NaOH] (w/v) ratio approached 2. The suspension was centrifuged (10000*g* for 5 min), and the supernatant and pellet fractions were separated.

Cellulose−ester dialysis membranes (MWCO: 6000−8000) from Spectra/Por Biotech (Spectrum Laboratories, Inc.) were boiled at 100 °C for 15 min and placed overnight at 4 °C in a 0.1 M Tris-HCl buffer (pH 7.4) before use. Supernatants containing alkali-soluble β-D-glucans and mannoproteins from yeast cell walls were dialyzed (1:100, v/v) with 0.02 M Tris-HCl buffer (pH 7.4) for at least 16 h at 4 °C with magnetic stirring. Mannans and β-D-glucans were separated on a concanavalin A Sepharose column (Pharmacia) at 4 °C for 3 h. Alkali-soluble β-D-glucans were eluted with 0.02 M Tris-HCl buffer (pH 7.4)/0.5 M NaCl and stored at −20 °C until use. Mannans were retained on the column.

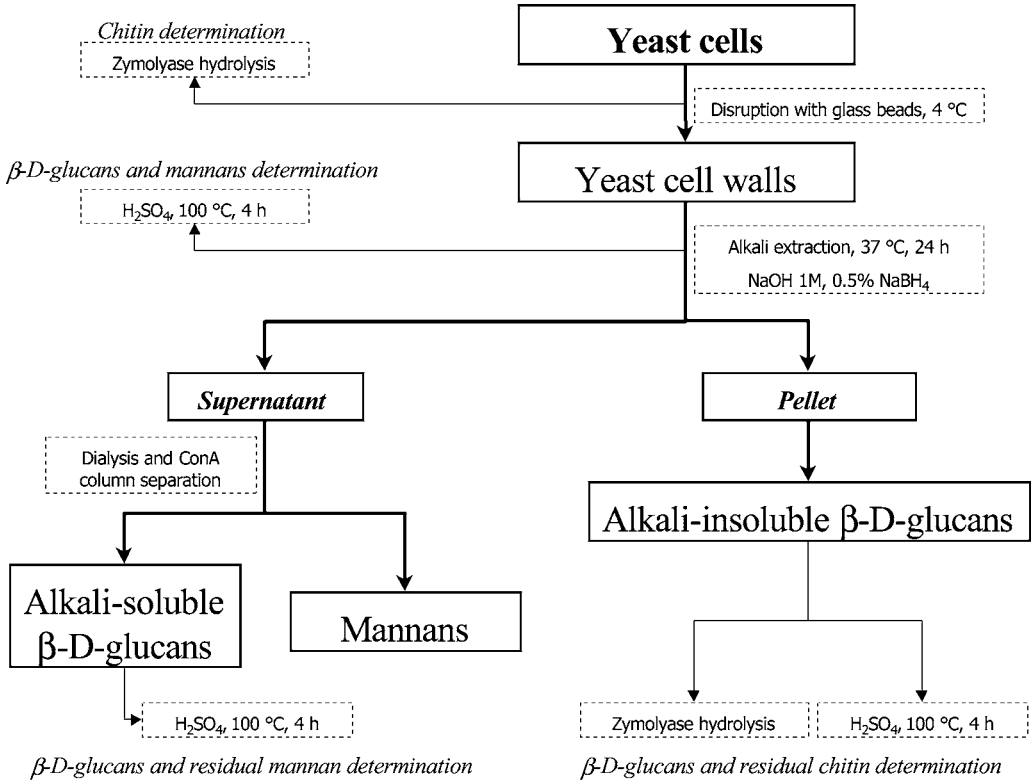

Figure 2. Diagram of the preparation procedure and analysis of yeast cell walls and extraction and analysis of alkali-soluble and alkali-insoluble fractions.

The pellets were thoroughly washed with 1 mL of 75% ethanol/10 mM Hepes buffer (pH 7.1) without suspending them. The pellets were then suspended in 2 mL of 0.1 M Tris-HCl buffer (pH 8.5) and stored −20 °C until use.

A Dionex Bio-LC system (Sunnyvale, CA) was used for quantitative analysis of cell wall carbohydrates with a pulsed amperometric detector equipped with a gold electrode. Cell wall carbohydrates were separated on a CarboPac PA1 anion-exchange column (4 × 250 mm) equipped with a CarboPac PA guard column. Elution was at room temperature at a flow rate of 1 mL/min with 18 mM NaOH. Analysis for the determination of cell wall components was carried out in triplicate. Chitin content was determined using an enzymatic method, and released glucosamine was quantified as described elsewhere (*25*).

Mycotoxin Quantification. ZEN was analyzed by isocratic HPLC on an HP-1090 series II HPLC (Hewlett-Packard Co.) using a UV diode array detector coupled to an HP-1046A fluorescence detector. Elution was on a C18 Nucleosil column (4 × 150 mm) equipped with a Spherisorb ODS-2 guard column (Macherey-Nagel GmbH and Co., Düren, Germany) at 50 °C and at a flow rate of 0.8 mL/min of acetonitrile. Twenty microliters of sample was injected by means of a six-port sample valve. UV detection was set at 280 nm, and the fluorescence detector at 280 nm (excitation) and 460 nm (emission) (*26*).

In Vitro Technique To Estimate the ZEN Complex-Forming Capacity of Yeast Cell Walls. The original in vitro technique used to study the complex-forming capacity of yeast cell walls for ZEN has been described by Yiannikouris et al. (*19*). For each in vitro test, 100 μg/mL of adsorbent was placed in tubes together with 2, 4, 6, 8, 10, or 20 μg/mL of ZEN dissolved in water. The tubes were agitated at 37 °C on a rotary shaker set at 200 rpm for 1.5 h and then centrifuged at 5000*g*. The supernatant fraction was then collected for free toxin analysis. The amount of bound toxin was calculated by subtracting the amount of free toxin found in the experimental tubes from the amount found in control tubes with no adsorbent.

Data Processing and Curve Fitting. Curves representing the amount of bound ZEN as a function of the amount of added ZEN were plotted according to Hill's equation, which improved fitting our experimental data compared to isothermal models, or sigmoid models with and without intercepting origin. Hill's equation, unlike other models, also integrates a factor accounting for the sigmoid shapes of the curve, which indicates a cooperative interaction between the toxin and the binder. Thus, Hill's model gives comprehensive information to explain the biological, physical, and chemical analysis of the adsorption process (*19*). DataFit 7.1 software (Oakdale Engineering) was used to plot the experimental data, set up the regression curve (curve fitting), and calculate the statistical data in the binding capacity tests. Hill's model with *n* sites (**Table 1**) was used to characterize the adsorption of ZEN on alkali-soluble and alkali-insoluble fractions obtained from each strain. Its graphic representation was a sigmoid plot of fractional saturation (*Y*), indicating a cooperative interaction. Hill's model was used to set up three submodels given in **Table 2**, each expressing the amount of bound toxin as a function of the total amount of toxin added to the medium [$T_{bound} = f(T_{total})$] and allowing the calculation of several parameters characterizing the interaction between components of yeast cell wall and ZEN (**Tables 1** and **2** and **Figure 3**). The association constant for the entire molecule (KD), the maximal amount of toxin bound (T^{max}_{bound}), the saturation point (K_{sat}), and the number of sites (n) were calculated. The HMN equation was used to evaluate individual adsorption capacities of alkali-soluble and alkali-insoluble fractions from each strain and to discriminate between strains according to their ZEN adsorption efficacy. Equation HMN-GT (**Table 2**) took into account the amounts of glucans in cell walls to evidence the interaction between β-D-glucan content and adsorption properties for ZEN. Finally, equation HMN-GA-S/IS took into account the respective amounts of alkali-

Table 1. Hill's Theoretical Model with *n* Sites Accounting for Biological Interactions[a]

theoretical biological basis		
Hill's model with *n* sites	$Y = \frac{[B]^n}{KD + [B]^n}$	$K_D = \sqrt[n]{KD}$

[a] Y = fractional saturation (concentration of sites on the binder that are actually occupied, divided by the total concentration of available sites); B = amount of free binder; KD = association constant for entire molecule; K_D = association constant per site; n = value related to the number of binding sites and used as a cooperativity indicator.

Table 2. Models Used To Plot and Evaluate ZEN Adsorption on β-D-Glucans of Yeast Cell Walls of *S. cerevisiae* According to Hill's Equation[a]

model expression: $T_{bound} = f(T_{total})$	
Hill's model with *n* sites (HMN)	$T_{bound} = \frac{T_{bound}^{max}(T_{total})^n}{KD_{total} + (T_{total})^n}$
Hill's model with *n* sites taking into account the amount of β-D-glucans (HMN-GT)	$T_{bound} = [\beta\text{-D-glucans}] \frac{T_{bound}^{max}(T_{total})^n}{[\beta\text{-D-glucans}]KD_{total} + (T_{total})^n}$
Hill's model with *n* sites taking into account the amount of alkali-soluble and alkali-insoluble β-D-glucans (HMN-GA-S/IS)	$T_{bound} = [\alpha] \times \frac{T_{bound}^{max}(T_{total})^n}{[\alpha] \times KD_{total} + (T_{total})^n}$ with $[\alpha] = ([S_{ol}] + [aI_{nsol}]) \times [\beta\text{-D-glucans}]$

[a] *a* = variable distinguishing the role played by alkali-insoluble compared with alkali-soluble β-D-glucans; I_{nsol} = amount of alkali-insoluble β-D-glucans (%); S_{ol} = amount of alkali-soluble β-D-glucans (%); KD_{total} = association constant compared with amount of toxins initially added; T_{bound} = amount of bound toxin (μg/mL); T_{total} = amount of total toxin added (μg/mL); T_{bound}^{max} = maximal amount of bound toxin (μg/mL).

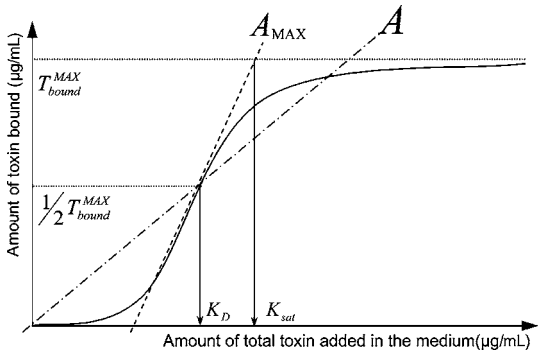

Figure 3. Curve of adsorption of a mycotoxin to an adsorbent with HMN. K_{sat} = saturation point (μg/mL), *A* = affinity rate (%), and A_{MAX} = maximal affinity (%).

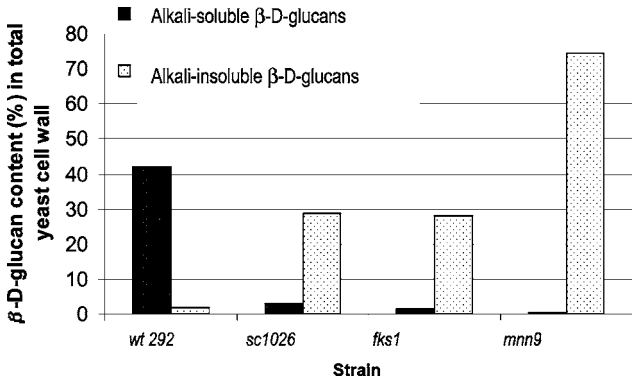

Figure 4. Alkali-soluble and alkali-insoluble β-D-glucan content in the cell wall of four strains of *S. cerevisiae*.

insoluble and alkali-soluble fractions in the total β-D-glucans and their respective roles in the ZEN adsorption process. β-D-Glucans were then calculated as follows: [(*a* × alkali-insoluble fraction) + alkali-soluble fraction], where *a* distinguished the role played by alkali-insoluble compared with alkali-soluble β-D-glucans. The affinity rates (A_{total}) relative to the total amount of ZEN toxin added to the medium were evaluated with the equation given below, where $K_{D,total}$ represents the association constant per site relative to the total amount of added toxin:

$$A_{total} = T_{bound}^{max}/2K_{D,total}$$

Statistical Analysis. Samples used for yeast cell wall composition were analyzed in triplicate to calculate means and standard deviations. Means were compared using the Tukey−Kramer multiple-comparisons test and GraphPad Instat 3.01 software system. The significance threshold was set at $p < 0.05$.

RESULTS AND DISCUSSION

Chemical Composition of β-D-Glucans of Yeast Cell Walls. **Figure 4** shows the distribution of the alkali-soluble and alkali-insoluble β-D-glucans. *Sc1026*, *fks1*, and *mnn9* presented high alkali-insoluble β-D-glucan contents, respectively 28.7, 28.2, and 74.5% of the whole yeast cell wall, whereas *wt292* contained only 1.7%. Conversely, *wt292* contained 42.0% of alkali-soluble β-D-glucans, whereas the other strains had <3%. The alkali extraction of cell walls produced two fractions containing >97% of β-D-glucans for each yeast strain, in agreement with the literature (*21*, *23*). Nevertheless, some trace residual mannans were found in the *wt292* alkali-soluble fraction and in the *sc1026* alkali-insoluble fraction. Residual chitin in *mnn9* represented 2.5% of the alkali-insoluble fraction, in agreement with results described elsewhere (*21*). Chitin is covalently linked to glucans, this association explaining the alkali-insolubility of β-D-glucans (*21*). Moreover, alkali-insolubility is also related to the spatial organization of β-D-glucans. These can adopt a triple helix form with a consequently greater resistance to alkali treatment (*21*, *23*). No chitin residue was detected in any alkali-soluble fraction.

Many studies have been conducted on the chemical structure of β-D-glucans and the organization of yeast cell walls. Cell walls are considered to be made up of different glucan types, depending on their solubility and extraction properties (*23*).

Adsorption of ZEN by Alkali-Soluble and Alkali-Insoluble Fractions of β-D-Glucans from Yeast Cell Walls Estimated in Vitro and Plotted with Hill's Model. As shown in **Table 4**, the R^2 and RSD values for both fractions were in the ranges of 0.88−0.99 and 0.111−0.655 μg/mL, respectively, showing the reliability of the HMN equation. The closest correlations were obtained with the alkali-insoluble fractions of *wt292*, *sc1026*, and *fks1* ($R^2 = 0.99$; RSD between 0.120 and 0.655 μg/mL). Adsorption parameters (**Table 4**) calculated with HMN according to the definitions given above (**Figure 3**; **Table 2**) showed little difference between the alkali-soluble fractions of the four strains. *Wt292*, *sc1026*, *fks1*, and *mnn9* had similar values for T_{bound}^{max} (between 2 and 3 μg/mL) and for *n* (~3). K_D (~7 μg/mL) and K_{sat} (~13 μg/mL) were identical for the alkali-soluble fractions extracted from *sc1026*, *fks1*, and *mnn9* and closely similar for *wt292* ($K_D = 6.6$ μg/mL; $K_{sat} = 8.8$ μg/mL). Finally, the affinity (*A* ranging from 14.8 to 17.3%) did not mark off the strains from each other. In contrast to these results obtained with the alkali-soluble fractions, the alkali-insoluble fractions from *wt292* and *mnn9* had greater adsorption properties ($p < 0.05$) than those from *sc1026* and *fks1*, with $T_{bound}^{max} = 7.1 \pm 1.1$ and 14.6 ± 4.6 μg/mL, $K_D = 9.8$ and 14.4 μg/mL, K_{sat}

Table 3. Regression Coefficients and Residual Standard Deviation (RSD, μg/mL) Calculated from HMN and HMN-GA-S/IS Equations for the Alkali-soluble and Alkali-insoluble Fractions of β–D-glucans Extracted from Yeast Cell Wall[a]

	wt292		sc1026		fks1		mnn9	
	R^2	RSD (ppm)	R^2	RSD (ppm)	R^2	RSD	R^2	RSD (ppm)
HMN: alkali-soluble fraction	0.948	0.289	0.980	0.161	0.955	0.266	0.991	0.111
HMN: alkali-insoluble fraction	0.989	0.237	0.989	0.655	0.989	0.120	0.884	0.345

	R^2	RSD
HMN-GT[b]	0.889	0.534
HMN-GA-S/IS[b]	0.969	0.296

[a] Each adsorption test on ZEN was done in aqueous medium with 100 μg/mL of *S. cerevisiae* cell walls in tubes placed at 37 °C for 1.5 h with orbital agitation. [b] HMN-GT and HMN-GA-S/IS equation included all four strains tested and took into account their total β-D-glucan contents or [(a × alkali-insoluble) + alkali-soluble] β-D-glucan contents.

Table 4. Adsorption Parameters Calculated with the HMN Equation for the Alkali-Soluble and Alkali-Insoluble Fractions of β-D-Glucans Extracted from Yeast Cell Wall[a]

	S. cerevisiae strain			
	wt292	sc1026	fks1	mnn9
	Extracted Alkali-Soluble β-D-Glucan Fraction			
n	5.94 ± 3.00a	3.41 ± 0.87a	2.79 ± 1.09a	3.35 ± 0.54a
T^{max}_{bound} (μg/mL)	2.08 ± 0.27a	2.33 ± 0.22ab	2.68 ± 0.45ab	2.59 ± 0.16b
K_D (μg/mL)	6.6	7.9	7.8	8.0
K_{sat} (μg/mL)	8.8	13.3	12.5	12.7
A (%)	15.8	14.8	17.3	16.3
	Extracted Alkali-Insoluble β-D-Glucan Fraction			
n	1.72 ± 0.34a	2.39 ± 0.23b	2.97 ± 0.52b	1.19 ± 0.26a
T^{max}_{bound} (μg/mL)	7.06 ± 1.14a	2.81 ± 0.51b	3.01 ± 0.52b	14.53 ± 4.62c
K_D (μg/mL)	9.8	7.2	6.3	14.4
K_{sat} (μg/mL)	21.3	6.8	12.0	38.6
A (%)	35.9	22.2	17.4	50.4

[a] Each adsorption test on ZEN was done with 100 μg/mL of *S. cerevisiae* cell walls in aqueous medium in tubes placed at 37 °C for 1.5 h with orbital agitation. K_{sat} = constant of saturation of the binding sites.

= 21.3 and 38.6 μg/mL, and A = 35.9 and 50.4% for the alkali-insoluble fractions from *wt292* and *mnn9*, respectively (**Table 4**). In addition, adsorption parameters of alkali-insoluble fractions of *sc1026* and *fks1*, ranging from 1.9 to 3.5 μg/mL for T^{max}_{bound}, from 6.3 to 8.0 μg/mL for K_D, from 6.8 to 13.3 μg/mL for K_{sat}, and from 14.8 to 22.2% for A, were close to those found for the alkali-soluble fractions of the four strains discussed previously.

It has been demonstrated for the whole cell wall (*16*, *19*) that the HMN model gives reliable results to estimate the adsorption properties of alkali-soluble and alkali-insoluble β-D-glucans for the four strains tested. The curves showing the amount of bound toxin in relation to the amount of total added toxin in the medium were of sigmoid shape (*19*), indicative of a cooperative interaction between either soluble or insoluble β-D-glucans with ZEN. Cooperativity has been considered to be a consequence of the dynamic 3D structure of the β-D-glucan network. As a matter of fact, NMR (*27*) and X-ray diffraction (*28*) investigations proved that β-D-glucans are organized in simple helix, which could be associated in triple-helix chains. Several triple-helix chains can also be associated in a complex network (*28*). The first bound molecules of ZEN open the helicoidal structure and so allow more molecules of toxin to be adsorbed until the binding sites are saturated (*16*). An n value of >1 indicates a strong cooperative effect, so the results given in **Table 4** show that the alkali-soluble fraction had a greater cooperativity than the alkali-insoluble fraction for *wt292* and *mnn9*. This result indicates that a greater accessibility of ZEN

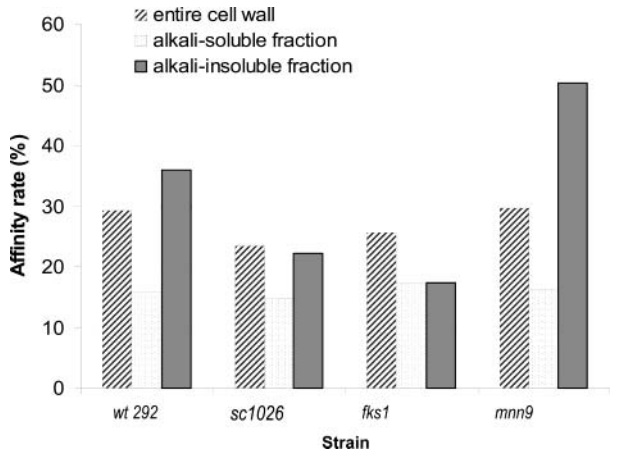

Figure 5. Affinity rate (%) of the same amount of whole cell wall and alkali-soluble and alkali-insoluble extracted β-D-glucans from four strains of *S. cerevisiae* toward ZEN.

to the adsorption sites of β-D-glucans occurs in the soluble fraction and that the highest amount of ZEN is adsorbed at the lowest concentrations.

The A values calculated with the alkali-insoluble β-D-glucans (**Figure 5**) and with the total β-D-glucan fraction in previous experiments (*16*) ranked the four tested strains in the same order. *Wt292* and *mnn9* had the highest affinities for both the alkali-insoluble fraction—respectively, 35.9−50.4%—and the total β-D-glucans—around 29%, whereas A values were between 17 and 23% for the alkali-insoluble fractions from *sc1026* and *fks1*, respectively. A values were under 17% for the alkali-soluble fractions of β-D-glucans derived from the four strains tested. The alkali-insolubility of β-D-glucans has a direct role in maintaining the rigidity and integrity of the yeast cell wall. β-D-Glucans also help to define a complex 3D structure with alternating regions of single helices and triple helices (*27*, *29*). In contrast, alkali-soluble β-D-glucans may make the yeast wall more flexible (*23*, *30*), inducing a greater cooperative activity (larger n value) than the alkali-insoluble fraction. Thus, we can conclude that differences observed between yeast strains on ZEN adsorption capacity are chiefly related to the insolubility and the complex 3D structure of the β-D-glucans in their cell walls.

β-D-Glucans in the cell wall of *S. cerevisiae* are mainly β(1,3)-D-linked glucose residues moderately branched unsubstituted β(1,6)-D-glucan chains (*18*, *23*, *31*, *32*). According to Fleet (*23*) and Shiota et al. (*32*), mutant strains of *S. cerevisiae* that are more susceptible to a β(1,3)-D-glucanase called zymolyase also have a smaller proportion of β(1,6)-D-linked residues in the alkali-insoluble fraction and a larger proportion of these linkages in the alkali-soluble glucans. Other studies using NMR

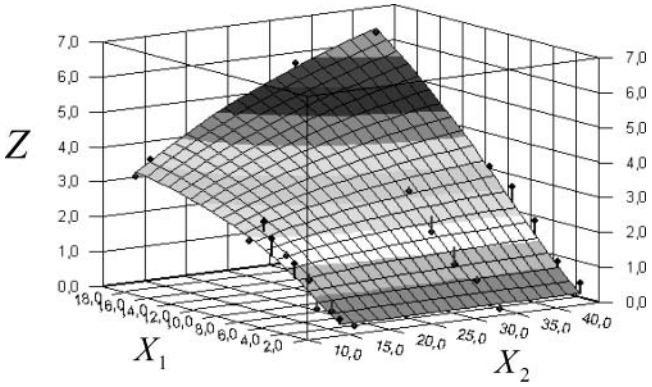

Figure 6. Graphic representation using HMN-GA-S/IS of the relationship between [(*a* × alkali-insoluble fraction) + alkali-soluble fraction] β-D-glucan content and the adsorption of ZEN. X_1 = amount of total ZEN added to the medium (μg/mL), X_2 = [alkali-soluble + alkali-insoluble] β-D-glucan content of the cell walls of the four strains tested (%), and Z = amount of ZEN adsorbed by yeast cell walls (μg/mL).

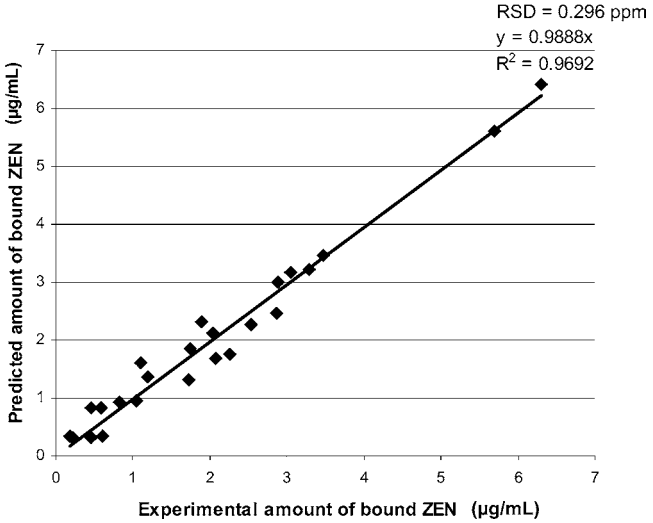

Figure 7. Regression between predicted data calculated with HMN-GA-S/IS and experimental data of the amount of ZEN adsorbed [the same amount of [(*a* × alkali-insoluble fraction) + alkali-soluble fraction] β-D-glucans (100 mg/mL) of each of the four strains of *S. cerevisiae* was added to the tubes during the in vitro adsorption test].

for nondestructive structural analysis of β(1,3−1,6)-D-linked glucans revealed that glucans can occur in linear and/or branched chains, independent of their solubility (*33*). It has also been established that β(1,6)-D-glucans are involved in the complexing of killer toxins (*23*). These findings, added to the complexing process proposed here, clearly show the importance of β-D-glucan molecules in interactive reactions.

Chitin content was partly eliminated during alkali extraction. *Mnn9* presented <2.5% chitin in the alkali-insoluble fraction, although it had 2−4 times more chitin in its cell wall than did the other three strains (**Figure 1**). This reduction of chitin content improved the capacity of the alkali-insoluble fraction of β-D-glucans to adsorb ZEN, *mnn9* showing 1.5 times more ability to complex ZEN than *wt292* (**Table 4**). In our previous study using the whole cell wall (*16*), no difference between these two strains in their affinity for ZEN was evidenced (A = 29.2 and 29.6% for *wt292* and *mnn9*, respectively), although *mnn9* had twice more β-D-glucan content in its cell walls than *wt292* These observations confirm the role played by chitin in the 3D conformation of β-D-glucan networks, which impairs the plasticity of the cell wall (*17, 34*). Also, these results evidence the major role played by the 3D structure of β-D-glucans in the ZEN adsorption process. Thus, a complex structure involving random coils and single- and/or triple-helix conformations for β-D-glucans favored adsorption by increasing binding site accessibility. The alkali-insoluble β-D-glucan fractions, which have more complex structures, exhibited greater A values than the simplified alkali-soluble fraction.

Role of Alkali-Soluble and Alkali-Insoluble β-D-glucans in ZEN Adsorption Evaluated by HMN-GA-S/SI. By eliminating the other components of the cell wall and estimating the impact of the additional effect of alkali-insoluble and alkali-soluble fractions in the model [(*a* × alkali-insoluble fraction) + alkali-soluble fraction] of β-D-glucans, we confirmed our previous results (*16*) indicating that high β-D-glucan content improved the ability of yeast cell walls to adsorb ZEN (**Figure 6**). HMN-GA-S/IS showed a greater impact on ZEN adsorption in the range of 6−20 μg/mL added ZEN in the medium and accounted for up to 98.9% of the experimental data (R^2 = 0.97, RSD = 0.296 μg/mL), whereas total β-D-glucans found in intact cell wall plotted with the HMN-GT equation accounted for only 96.2% (R^2 = 0.89, RSD = 0,534 μg/mL) (**Table 3**; **Figure 7**). The mean value of n was 1.5 (**Table 5**), indicating a strong cooperativity during ZEN complexing. Calculated values for

Table 5. Contribution of [(a × Alkali-Insoluble + Alkali-Soluble] β-D-Glucan Content in the in Vitro Test for ZEN Adsorption Estimated According to HMN-GA-S/SI[a]

$$T_{bound} = [\alpha] \times \frac{T^{max}_{bound}(T_{total})^n}{[\alpha] \times KD_{total} + (T_{total})^n}$$

with $[\alpha] = ([S_{ol}] + [a I_{nsol}]) \times [\beta\text{-D-glucans}]$

R^{2a}	n	T^{max}_{bound} (ppm)	KD (ppm)	a
0.969 (RSD = 0.296)	1.57 ± 0.12	0.30 ± 0.03	2.60 ± 0.51	0.45 ± 0.06

[a] T^{max}_{bound}, KD, and n are expressed per unit of β-D-glucan.

T^{max}_{bound} and KD_{total} expressed per unit of β-D-glucans were 0.30 ± 0.03 and 2.60 ± 0.51 μg/mL, respectively. Because the roles played by the alkali-soluble and alkali-insoluble fractions were different (**Table 4**), parameter a was used in the equation to take into account the difference in adsorption abilities of the two fractions. Thus, as a was <1 (a = 0.45 ± 0.06), the role played by the alkali-soluble fraction was more significant in ZEN adsorption than that played by the alkali-insoluble fraction.

The importance of β-D-glucans in the whole yeast cell wall, using the HMN-GT equation, was evidenced in a previous study (96.2% of the experimental data accounted for, R^2 = 0.90; **Table 3**), but some artifacts were observed because of the use of whole cell wall, which also contained mannans and chitin (*16*). The HMN-GA-S/IS equation made using Hill's equation more relevant by increasing the close relationship between β-D-glucans extracted from yeast cell walls and their ability to adsorb ZEN. Thus, calculated values for T^{max}_{bound} and KD_{total} expressed per unit of β-D-glucans (**Table 5**) were greater with HMN-GA-S/SI than those previously found with HMN-GT, 0.30 ± 0.03 and 2.60 ± 0.51 with the former compared with 0.20 ± 0.05 and 1.50 ± 0.51 with the latter, respectively. In addition, as observed previously with HMN-GT, n remained equal to 1.5, indicating a strong cooperativity during the adsorption process.

The results characterizing the impact of both [(*a* × alkali-insoluble) + alkali-soluble] fractions in their adsorptive abilities (a = 0.45 ± 0.06) could be explained by the difference in cell wall composition among yeast strains. As shown before (**Figure 1**), strains did not present the same amounts of β-D-glucans in their cell walls. *Wt292* and *mnn9* strains had larger glucan

contents than *sc1026* and *fks1*, and *mnn9* had twice as much glucan as *wt292*. Also, glucans of *mnn9*, *fks1*, and *sc1026* were mainly composed of alkali-insoluble β-D-glucans, whereas glucans of *wt292* were made of highly alkali-soluble β-D-glucans (**Figure 4**). Focusing on *sc1026* and *fks1* strains, alkali-insoluble β-D-glucans represented >90% of the total β-D-glucan content; conversely, *wt292* had 96.2% alkali-soluble β-D-glucans in its total β-D-glucan content and concomitantly also had the highest adsorptive ability for ZEN when [($a \times$ alkali-insoluble) + alkali-soluble] fractions are considered (**Figure 6**). Thus, alkali-soluble β-D-glucans had greater impact in adsorption than alkali-insoluble β-D-glucans, when the total β-D-glucan composition of the four strains is considered. *Mnn9* had greater adsorptive capacity owing to its larger total β-D-glucan content compared with *wt292* (80 and 44%, respectively) and also a high alkali-insoluble β-D-glucan content in its cell wall (74.3%) compared with the alkali-soluble β-D-glucan content of *wt292* (42.0%). Nevertheless, adsorptive properties of alkali-soluble fractions did not vary among strains, whereas alkali-insoluble fractions still played the main role in discriminating among the four strains tested.

From the results obtained with individual fractions or with HMN-GA-S/SI plotting, we can conclude that yeast strains that are highly effective ZEN adsorbers will be strains with a large quantity of β-D-glucans in their cell walls and a low chitin content. Glucans will be mostly composed of alkali-insoluble β-D-glucans (high affinity and high T_{bound}^{max}) with a complex, densely branched, 3D architecture, thus possessing a large number of binding sites. Glucans will be composed of a smaller but still significant proportion of alkali-soluble β-D-glucans that enhance the cooperative process and allow a high accessibility to the adsorptive sites (high *n* value) for low concentrations of ZEN.

Because the alkali-insoluble fraction represents the main discriminating component in ZEN adsorption, we suggest that the in vitro adsorption technique with HMN modeling and alkali extraction could be used as a screening test to evaluate the efficacy of yeast strain cell walls as mycotoxin adsorbents.

This work clearly underscores the major role played by β-D-glucans in yeast cell walls and their alkali-extracted fractions and the importance of their three-dimensional conformation during the adsorption of ZEN. In many respects to inorganic adsorbents, such compounds could thus be used to limit the bioavailability of mycotoxins in the digestive tract of animals and reduce the hazard of absorbing contaminated edible food or feed, without adversely affecting the environment when excreted.

SAFETY

Zearalenone, like all mycotoxins, is a hazardous chemical and must be handled with extreme care. Protective clothing, gloves, a fume hood, and goggles are essential to prevent exposure to mycotoxins.

ABBREVIATIONS USED

a, variable distinguishing the role played by alkali-insoluble compared with alkali-soluble β-D-glucans; *A*, affinity rate; *B*, amount of free binder; HMN, Hill's model with *n* sites; HMN-GT, Hill's model with *n* sites with factor proportional to the total β-D-glucan content; HMN-GA-S/IS, Hill's model with *n* sites with factor proportional to the alkali-soluble and alkali-insoluble β-D-glucan content composition; I_{nsol}, alkali-insoluble β-D-glucans; K_D, association constant per site; KD, association constant per unit of β-D-glucans; K_{sat}, constant of saturation of the binding sites; *n*, value related to the number of binding sites and cooperativity indicator; S_{ol}, alkali-soluble β-D-glucans; T_{bound}, amount of bound toxin; T_{bound}^{max}, maximal amount of bound toxin; T_{total}, amount of total toxin added; *Y*, fractional saturation; ZEN, zearalenone.

ACKNOWLEDGMENT

We especially thank Alltech Inc. for supplying the industrial *sc1026*. We thank Xavier Cameleyre (Critt Bio-Industries, INSA, Toulouse, France) for helpful support in the HPLC methods of ZEN quantification and Pierre Galtier (INRA-UR66, Toulouse, France) for helpful personal involvement in the setting up of this research.

LITERATURE CITED

(1) CAST. *Mycotoxins: Risks in Plant, Animal, and Human Systems*; Task Force Report 139; Niyo, K., Ed.; Council for Agricultural Science and Technology: Ames, IA, 2003; pp 1−199.

(2) Yiannikouris, A.; Jouany, J.-P. Mycotoxins in feeds and their fate in animals: a review. *Anim. Res.* **2002**, *51*, 81−99.

(3) Saenz de Rodriguez, C. A.; Bongiovanni, A. M.; Borrego, L. C. d. An epidemic of precocious puberty in Puerto Rican children. *J. Pediatr.* **1985**, *107*, 393.

(4) Harvey, R. B.; Healing, G.; Rees, S. J.; Everett, D. J.; Cockburn, A. Glucocorticosteroid interactions with natural toxins: a mini review. *Nat. Toxins* **1994**, *2*, 341−346.

(5) Kurtz, H. J.; Mirocha, C. J. Zearalenone (F2) induced estrogenic syndrome in swine. In *Mycotoxic Fungi, Mycotoxins, Mycotoxicoses*; Wyllie, T. D., Morehouse, L. G., Eds.; Dekker: New York, 1978; pp 1256−1264.

(6) Sydenham, E. W.; Thiel, P. G.; Marasas, W. F. O. Occurrence and chemical determination of zearalenone and alternariol monomethyl ether in sorghum-based mixed feeds associated with an outbreak of suspected hyperestrogenism in swine. *J. Agric. Food Chem.* **1988**, *36*, 621−625.

(7) Chang, K.; Kurtz, H. J.; Mirocha, C. J. Effects of the mycotoxin zearalenone on swine reproduction. *Am. J. Vet. Res.* **1979**, *40*, 1260−1267.

(8) Forsell, J. H.; Pestka, J. J. Relation of 8-ketotrichothecene and zearalenone analogue structure to inhibition of mitogen-induced human lymphocyte blastogenesis. *Appl. Environ. Microbiol.* **1985**, *50*, 1304−1307.

(9) Luster, M. I.; Boorman, G. A.; Korach, K. S.; Dieter, M. P.; Hong, L. Mechanisms of estrogen-induced myelotoxicity: evidence of thymic regulation. *Int. J. Immunopharmacol.* **1984**, *6*, 287−297.

(10) Pasikatan, M. C.; Dowell, F. E. Sorting systems based on optical methods for detecting and removing seeds infested internally by insects or fungi: a review. *Appl. Spectrosc. Rev.* **2001**, *36*, 399−416.

(11) Jemmali, M. Decontamination and detoxification of mycotoxins. *J. Environ. Pathol. Toxicol. Oncol.* **1990**, *10*, 154−159.

(12) Karlovsky, P. Biological detoxification of fungal toxins and its use in plant breeding, feed and food production. *Nat. Toxins* **1999**, *7*, 1−23.

(13) Scott, P. M. Industrial and farm detoxification processes for mycotoxins. *Rev. Med. Vet.* **1998**, *149*, 543−548.

(14) Dawson, K. A.; Evans, J.; Kudupoje, M. Understanding the adsorption characteristics of yeast cell wall preparations associated with mycotoxin binding. In *Science and Technology in the Feed Industry*; Lyons, T. P., Jacques, K. A., Eds.; Nottingham University Press: Nottingham, U.K., 2001; pp 169−181.

(15) Devegowda, G.; Raju, M. V. L. N.; Afzali, N.; Swamy, H. V. L. N. Mycotoxin picture world-wide: novel solutions for their counteraction. In *Biotechnology in the Feed Industry*; Lyons, T. P., Jacques, K. A., Eds.; Nottingham University Press: Nottingham, U.K., 1998; pp 241−256.

(16) Yiannikouris, A.; François, J.; Poughon, L.; Dussap, C.-G.; Bertin, G.; Jeminet, G.; Jouany, J.-P. Adsorption of zearalenone by β-D-glucans in the *Saccharomyces cerevisiae* cell wall. *J. Food Prot.* **2004**, *67*, in press.

(17) Kollar, R.; Reinhold, B. B.; Petrakova, E.; Yeh, H. J. C.; Ashwell, G.; Drgonova, J.; Kapteyn, J. C.; Klis, F. M.; Cabib, E. Architecture of the yeast cell wall. β(1,6)-D-glucan interconnects mannoprotein, β(1,3)-D-glucan, and chitin. *J. Biol. Chem.* **1997**, *272*, 17762−17775.

(18) Manners, D. J.; Masson, A. J.; Patterson, J. C. The structure of a β(1,3)-D-glucan from yeast cell walls. *Biochem. J.* **1973**, *135*, 19−30.

(19) Yiannikouris, A.; Poughon, L.; Cameleyre, X.; Dussap, C.-G.; François, J.; Bertin, G.; Jouany, J.-P. A novel technique to evaluate interactions between *Saccharomyces cerevisiae* cell wall and mycotoxins: application to zearalenone. *Biotechnol. Lett.* **2003**, *25*, 783−789.

(20) Grant, P. G.; Phillips, T. D. Isothermal adsorption of aflatoxin B1 on HSCAS clay. *J. Agric. Food Chem.* **1998**, *46*, 599−605.

(21) Nguyen, T. H.; Fleet, G. H.; Rogers, P. L. Composition of the cell walls of several yeast species. *Appl. Microbiol. Biotechnol.* **1998**, *50*, 206−212.

(22) Dallies, N.; François, J.; Paquet, V. Yeast functional analysis reports: a new method for quantitative determination of polysaccharides in the yeast cell wall. Application to the cell wall defective mutants of *Saccharomyces cerevisiae*. *Yeast* **1998**, *14*, 1297−1306.

(23) Fleet, G. H. Chapter 5. Cell walls. In *The Yeasts*; Rose, A. H., Harrison, J. S., Eds.; Academic Press: London, U.K., 1991; pp 199−271.

(24) Catley, B. J. Chapter 8. Isolation and analysis of cell walls. In *Yeast; a Practical Approach*; Campbell, D. J. H., Ed.; IRL Press: Oxford, WA, 1988; pp 163−183.

(25) Popolo, L.; Gilardelli, D.; Bonfante, P.; Vai, M. Increase in chitin as an essential response to defects in assembly of cell wall polymers in the ggp1delta mutant of *Saccharomyces cerevisiae*. *J. Bacteriol.* **1997**, *179*, 463−469.

(26) Lauren, D. R.; Agnew, M. P. Multitoxin screening method for *Fusarium* mycotoxins in grains. *J. Agric. Food Chem.* **1991**, *39*, 502−507.

(27) Kogan, G. Bioactive natural products (part D): β(1,3)- and β(1,6)-D-glucans of yeasts and fungi and their biological activity. In *Studies in Natural Products Chemistry*; Atta-ur-Rahman, Ed.; Elsevier Science: Karachi, Pakistan, 2000; pp 107−151.

(28) Chuah, C. T.; Sarko, A.; Deslandes, Y.; Marchessault, R. H. Packing analysis of carbohydrates and polysaccharides. Part 14. Triple-helical crystalline structure of curdlan and paramylon hydrates. *Macromolecules* **1983**, *16*, 1375−1382.

(29) Lipke, P. N.; Ovalle, R. Cell wall architecture in yeast: new structure and new challenges. *J. Bacteriol.* **1998**, *180*, 3735−3740.

(30) Kopecka, M.; Phaff, H. J.; Fleet, G. H. Demonstration of a fibrillar component in the cell wall of the yeast *Saccharomyces cerevisiae* and its chemical nature. *J. Cell. Biol.* **1974**, *62*, 66−76.

(31) Manners, D. J.; Masson, A. J.; Patterson, J. C.; Björndal, H.; Lindberg, B. The structure of a β(1,6)-D-glucan from yeast cell walls. *Biochem. J.* **1973**, *135*, 31−36.

(32) Shiota, M.; Nakajima, T.; Satoh, A.; Shida, M.; Matsuda, K. Comparison of β-D-glucan structures in a cell wall mutant of *Saccharomyces cerevisiae* and the wild type. *J. Biochem.* **1985**, *98*, 1301−1307.

(33) Kim, Y.-T.; Kim, E.-H.; Cheong, C.; Williams, D. L.; Kim, C.-W.; Lim, S.-T. Structural characterization of β(1,3)-, β(1,6)-linked glucans using NMR spectroscopy. *Carbohydr. Res.* **2000**, *328*, 331−341.

(34) Kollar, R.; Petrakova, E.; Ashwell, G.; Robbins, P. W.; Cabib, E. Architecture of the yeast cell wall. The linkage between chitin and β(1,3)-D-glucan. *J. Biol. Chem.* **1995**, *270*, 1170−1178.

Received for review October 2, 2003. Revised manuscript received January 16, 2004. Accepted March 10, 2004. This work was co-supported (CIFRE No. 704/2000) by Alltech Co., ANRT (Association Nationale de la Recherche Technique), and INRA.

JF035127X